

Comparison among chemical and electromagnetic stirring and vibration melt treatments for Al–Si hypereutectic alloys

F.C. Robles Hernández^{a,*}, J.H. Sokolowski^b

^a Transportation Technology Center Inc., Pueblo, CO 81001, USA

^b LMCT Group, University of Windsor, Essex Hall, Room 212A, 401 Sunset Avenue, Windsor, Ont., Canada N9B 3P4

Received 28 September 2005; received in revised form 1 September 2006; accepted 2 September 2006

Available online 17 October 2006

Abstract

A comparison among the microstructure refinement between chemical treatment and electromagnetic stirring and vibration (ESV) for the 390 Al–Si hypereutectic alloys is presented. The use of melt treatments assisted by chemical (i.e. P and Sr) modifiers for Al–Si hypereutectic alloys are limited to reduce in size the primary Si particles by the multiplication of active nuclei sites (Si agglomerates). This limits the coarsening effect of the primary Si particles in the liquid state. This paper shows the microstructures of ESV melt treated of Al–Si hypereutectic alloys; such microstructures show that ESV melt treatments are effective in the liquid and semi-solid states. In this paper are presented microstructures of ESV melt treated samples at temperatures as high as 130 °C above the liquidus. ESV treatments applied at temperatures of 100 °C above liquidus or higher have a limited effectiveness in Si modification by promoting the formation of feathered-like primary Si particles. ESV treatments are more effective when applied at temperatures close to liquidus (i.e. 620 °C for the 390 Al–Si alloy), under this condition ESV treatments can successfully modify primary Si particles transforming them into “eutectic-like” particles. The resulting microstructure shows primary Si free microstructures with similar appearance to a Sr modified Al–Si hypoeutectic microstructure. The use of combined ESV and chemical treatments further refining the microstructure of the Al–Si hypereutectic alloys. In the present paper, the Si modification level was quantified using the silicon modification level (SiML). Thermal analysis results show good agreement with microstructure refinement, showing a correlation of $R^2 = 0.89$.

© 2006 Elsevier B.V. All rights reserved.

Keywords: Microstructure; Thermal analysis; Metallography; Al–Si hypereutectic alloys; Metals and alloys; Electromagnetic stirring and vibration

1. Introduction

Aluminium alloys are considered the most abundant, thus important, after steel due to their light weight, physical and mechanical characteristics [1]. Among the aluminium alloys the aluminium silicon (Al–Si) with 5–11 wt% Si with additions of Mg, Ni and Cu are the most widely used. Al–Si alloys have shown good performance mainly for aerospace and automotive applications [1–3]. Microstructure refinement is used to boost the mechanical properties and characteristics of Al–Si alloys and have been successfully applied by chemical agents (Si modifiers and grain refiners), semi-solid processing, mechanical or electromagnetic stirring, rehocasting and thixocasting means [2–18].

Al–Si hypereutectic alloys (with more than 12.6 wt% of Si) are attractive as a substitute for cast iron due to their high wear resistance, lower density, higher thermal stability, corrosion resistant, thermal conductivity, heat treatment capabilities, machining, etc. However, their main limitation is the presence of coarse and brittle primary Si particles that easily crack exposing the soft aluminium matrix to extreme wear. The VEGA2300 engine is a good example; for instance, it was the first attempt to eliminate cast iron cylinder liners by producing an engine block of Al–Si hypereutectic alloy [19,20]. The coarse and brittle primary Si particles are presumably the reasons for the VEGA2300 engine to be removed from production.

The characteristics of the liquid state of pure element and alloys has been widely studied and has been reported that some elements and alloy systems present short to medium range atomic arrangements [21–29]. The determination of nanometric or micrometric domains of ordered atoms in the liquid state are known as “agglomerations of atoms”. These atomic arrangements became smaller as the temperature increases but they also

* Corresponding author. Tel.: +1 905 678 2977; fax: +1 514 370 3310.

E-mail address: fcrh20@yahoo.com (F.C. Robles Hernández).

¹ Formerly at the Light Metals Casting Technology (LMCT) Group at the University of Windsor and recently hired by the Transportation Technology Center Inc., Pueblo, CO. 81001 USA.

Nomenclature

AC	alternating currents
B_0 and B_t	magnetic flux density in the centre of the coil for the AC or DC field(s) (T)
DC	direct currents
ESV	electromagnetic stirring and vibration
F	Lorentz force (N/m^2)
H	magnetic field strength (At/m)
I	AC and/or DC current (At/m)
J	current density (A/m^2)
k	equilibrium distribution coefficient or partition coefficient parameter
N	number of turns of the electromagnetic coil
P	electromagnetic vibrating pressure (MPa)
SiML	silicon modification level
$T_{\text{E,NUC}}^{\text{Al-Si}}$	Al–Si eutectic nucleation temperature
T^{Casting}	pouring or casting temperature (usually 150–200 °C above liquidus)
T^{LIQ} and ΔT^{LIQ}	liquidus temperature and its respective undercooling
$\Delta T_{\text{E}}^{\text{Al-Si}}$	characteristic undercooling for the Al–Si eutectic reaction

Greek letters

Φ_{INT} , Φ_{EXT}	internal and external diameter for the electromagnetic coils
Φ_{UPPER}	upper diameter for the stainless steel crucible
α and β	geometrical parameters of the electromagnetic coil
μ_0 and μ_r	absolute and relative magnetic permeability (in T/A m)
ω	angular frequency (rad)

coarse as the temperature of the melt approaches liquidus. The Si agglomerates have been identified by X-ray diffraction in liquid alloys (i.e. Al–11 to 13 wt% Si alloys) at temperatures as high as 1075 °C and other techniques including optical microscopy [23–25]. Using high temperature melting techniques assisted by plasma was found that by melting Al–Si hypereutectic alloys at high temperatures it is possible to eliminate the Si agglomerates. This result in a refinement mechanism and the microstructures of the casting treated using this method presents refined Si particles [28].

Recently, Xiunfang et al. [21] and Robles Hernandez et al. [4,23,24] investigated the effect of chemical modification (using Sb) [21] and electromagnetic stirring and vibration (ESV), respectively, on Al–Si eutectic and hypereutectic alloys in the liquid state. The use of Sb promotes the formation of the agglomerates increasing the number of active sites for nucleation resulting in a microstructure refining effect. Unfortunately, this method is limited to the reduction in size of the final primary Si particles [21]. The use of the ESV technique has proven to be the most successful method to refine Al–Si alloys such as the 390 from the liquid state [4]. In addition, it was reported that the

Si agglomerates growth linearly as the temperature decreases and below the liquidus temperature they transform into primary Si particles following the same growth path [23,24].

In the present paper are presented the results of ESV and chemical treatments conducted in the liquid and semi-solid states to refine the microstructure of the Al–Si hypereutectic alloys in particular the coarse primary Si. Different melt treatments were conducted using chemical modification (adding P and Sr), electromagnetic stirring and vibration and a combination of the ESV with P and Sr additions. The ESV melt treatments were conducted at different temperatures. The main goal is to conduct the treatments in such way that are concluded at temperatures close to liquidus. During the solidification process thermal analysis was conducted in order to identify the effect of melt treatments and solidification behaviour. The resulting samples were analyzed by optical microscopy and an analogy among thermal analysis and the microstructures is discussed.

2. Experimental procedure

Charges of 12 kg of the 390 Al–Si alloy were melted at a temperature of 200 °C above liquidus (casting temperature). The liquidus temperature for the investigated alloy was determined using the silicon equivalent (Si_{EQ}) methodology [21] that is a highly accurate method based on the alloy's chemical composition (Table 1). Once the melt reached the casting temperature the degassing operation was conducted by blowing Ar through a rotating graphite impeller for 20 min at a rate of 1 dm³/s.

The electromagnetic stirring and vibration treatments were carried out at various temperatures, but in all cases were initiated above liquidus temperatures. Some of the treatments were ended above and some below the liquidus temperature. The ESV + chemical treatments were conducted in the range of temperatures from 700 to 600 °C. The chemical modifiers added to the melt were 60 ppm of P and 60 ppm of Sr using the Cu–8 wt% P and Al–5 wt% Sr master alloys correspondingly. The Cu–8 wt% P was added at the casting temperature then a 10 min period was allowed as an incubation time for P; as recommended in references [16–18]. Sr was added a few seconds after the melt reached the liquidus temperature (during solidification) since the effect of Sr is primarily the refinement of the Al–Si eutectic particles; in addition, Sr reacts rapidly. Mulazimoglu and Gruzleski [31] reported that combined additions of P and Sr have positive effects on Si modification for Al–Si alloys containing up to 14 wt% Si that is similar in composition with the alloy used in this investigation (see Table 1).

Fig. 1 shows the schematic workstation where the ESV melt treatments were conducted in the present investigation. The AC and DC coils were similar with the following characteristics: 120 turns, using a flat Cu wire of 0.1 cm², $\Phi_{\text{EXT}} = 22$ cm, $\Phi_{\text{INT}} = 9.5$ cm, length = 4.2 cm. The coils were located one on top of each other with a gap in between of 0.5 cm. This gap was designed to release heat more easily allowing the Joulean heat generated to be released more rapidly the cooling of the coils is assisted by a custom made coil cooling system. The coils were designed for extreme environment conditions and stands

Table 1
Chemical composition and liquidus temperature (T_{LIQ} , °C) of the 390 Al–Si alloy as determined by optical emission spectroscopy (OES) and Si_{EQ} , respectively [21]

Element (wt%)									T_{LIQ} (°C)
Si	Cu	Fe	Mg	Mn	Zn	Ti	Ni	Sn	
15.4	3.0	0.6	0.6	0.3	0.6	0.07	0.6	0.01	629.7

Alloying elements that have effect on microstructure refinement (such as P, Sr, Na, Ca, Sb, and other alkaline or rare earth elements) were kept below traces it means <0.001 wt%. Except for samples that were chemically treated.

temperatures of up to 200 °C, therefore a thermocouple was introduced between the coils to monitor their temperature allowing full control for safe working conditions.

The DC magnetic field was placed in the sample in the upwards direction in order to avoid a vortex that can introduce air or impurities into the melt that will result detrimental for the casting's service characteristics. For all the experiments were used a frequency for the AC current of 100 Hz and 100 A for both, AC and DC, electromagnetic fields. In literature [4] reports the above-conditions as optimum for ESV melt treatments for Al–Si hypereutectic alloys.

The crucible used was engineered for the purposed of this research using 304 non-magnetic stainless steel eliminating interactions between the magnetic fields and the crucible. The dimensions of the crucible are as follows: length = 9 cm, $\Phi_{UPPER} = 9$ cm with a taper angle of 5° for easy extraction of the sample. Between the crucible and the electromagnetic coils ceramic insulation was placed. This crucible has ~300 mL capacity that is equivalent to 700 g of molten 390 alloy. In the centre of the sample a K thermocouple was introduced to record the cooling curves.

3. Results and discussions

In following are presented the main ESV treatment parameters and the algorithms used for their determination [4,11,12]:

$$B = \frac{\mu_0 I N}{h(b-a)} a \beta \ln \frac{\alpha + \sqrt{a^2 + b^2}}{1 + (1 + \beta^2)^2} \quad \beta = \frac{h}{2a}; \quad \alpha = \frac{b}{a} \quad (1)$$

The calculated magnetic field intensity based on the configuration of the coils used on this research are $B_0 = B_t = 0.1$ T for the AC and DC magnetic fields, respectively. The alternating magnetic field in a liquid melt generates Eddy currents and thus a Lorentz force that can be determined as follows $F = J \times B_t$, which is a time independent component with a frequency of $2N$ (where N is the number of cycles). The interaction of the stationary magnetic field (B_0) and the induced AC current creates a vibration with a frequency of $2N$. The vibration is produced in the exterior of the molten sample (see Fig. 1) that corresponds to

the section where the Eddy currents are formed that is also the section where the interaction among the AC and DC magnetic fields occurs.

The DC magnetic field covers the entire sample (Eq. (2)). The section covered for the AC field is known as skin effect and has known deep of penetration (δ) based on the characteristics of the sample and AC current (Eq. (2)). The deep of penetration can be manipulated depending on the conductivity ($\sigma_0 = 5.1 \times 10^6 \Omega/m$ for liquid aluminium at 660 °C), melt temperature, density of the melt, alloy composition and frequency of the ac current. It is obviously the frequency of the AC current the variable that can be easily manipulated thus in previous experiments it was used to determine its optimum value and set as 100 Hz for the 390 Al–Si alloy [4].

The control of the frequency of the electrical current can lead to the following effects: a high frequency for the AC current reducing the deep of penetration (Eq. (2)). Therefore, the Eddy currents density and the Lorentz forces are increased, this build up localized pressure that result in more severe ESV conditions. However, this can create highly turbulent flow of the melt and large amount of heat (*Joulean*) in the system making it work as an induction heater rather than a melt treatment station. Additionally, the internal corners of the electromagnetic coils will work under extreme conditions with the possibility to seriously damage the coils (Fig. 1 “hot spots”) that can result catastrophic.

The opposite procedure, low frequency for the AC current, will permit a more homogeneous distribution of the AC field among the sample but at the same time will reduce the Eddy currents density creating weaker pressure pulses and in order to have similar effects on microstructure considerably higher currents will be required (Eqs. (3) and (4)). Therefore, full control of these variables is required to assess the optimum ESV melt treatment conditions. In following are provided the

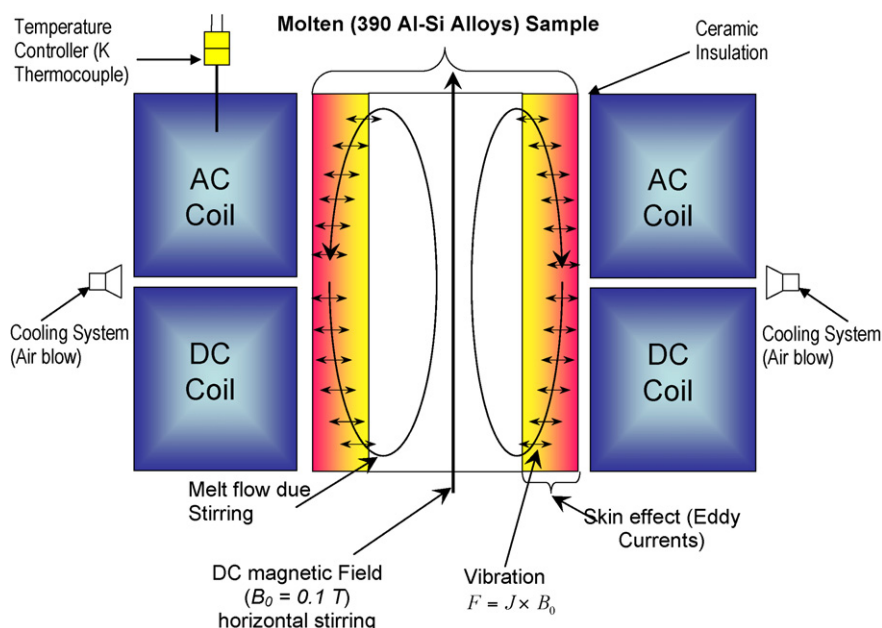


Fig. 1. Scheme of the electromagnetic stirring and vibration (ESV) workstation and the interaction of the imposed AC and DC magnetic fields on the liquid melt during melt treatment.

equations used to determine the deep of penetration (δ), density of the Eddy currents (J_m) and electromagnetic vibrating pressure:

$$\delta = \sqrt{\frac{2\rho}{\sigma_0\mu_0\omega}} \quad (2)$$

$$J_m \approx \frac{\sqrt{2}}{\delta} \frac{H_m}{\sqrt{r/r_2}} \exp\left(\frac{r-r_2}{\delta}\right) \quad (3)$$

$$H_m = \sqrt{2}I\omega$$

$$P = \frac{B_0IF}{a} \sin \omega t \quad (4)$$

The deep of penetration for the current investigation at a temperature of 660 °C was $\delta = 28.8$ mm, the respective density for the Eddy current was $J_m = 4.9 \times 10^6$ A/m² that resulted in a peak pressure of $P = 4.035$ MPa. A full control of the above-calculated parameters is crucial to assess a desired refinement of the microstructure. The use of different dimensions for the electromagnetic coils can also decrease the required optimum current ESV melt treatments. In this research the dimension were optimized based on the sample's dimensions and casting requirements; the workstation used in this research has as a main goal to conduct melt treatments for samples to cast pistons and cylinder liners, the results of this investigations are contemplated in future research papers.

The metallographic observations of the reference sample (untreated) of the 390 alloy present a modification free microstructure and is mainly composed by coarse primary Si particles, Al–Si/Al–Mg/Al–Cu/Al–Ni eutectics Fe and Pb phases (Fig. 2). All phases in the microstructure of the reference sample are coarse showing similar characteristics as the commercial and industrially used 390 alloy [1].

Some of the primary Si particles observed in the ESV treated samples at temperatures as high as 100 °C above the liquidus present a feathered morphology and the rest of the primary Si remain unmodified. Fig. 2 shows the micrographs of all the ESV treated and ESV + chemically modified samples at various temperatures. It is possible that the feathered morphology is a non-refined primary Si particle that was forced to solidify in a semi-regular eutectic-like structure by the effect of vibration. Gruzleski [1] reported that the semi-regular eutectic nucleation is characteristic of different solidification conditions, which greatly influence the microstructure. Extrapolating this concept to the actual ESV melt treatment conditions can be translated that the combined effect of stirring and vibration can result in a non-homogeneous solidification conditions. A higher level of refinement of the microstructure was observed in samples ESV treated at temperatures close to liquidus as shown in Fig. 2. The level of refinement was determined using the SiML standard [30].

From Fig. 2 can be observed that two parameters have major influence in Si modification, one is the temperature at which the melt treatment is applied and the other is the chemical modifiers. It is, for instance, important to notice that the highest level of modification for ESV treated samples (no chemical modifications) was reached on melt treatments concluded at temperatures

close to liquidus, it means approximately 620 °C. Actually, it was found that ESV treatments terminated around 620 °C have primary Si free microstructures (Fig. 2). It is the primary Si particles were refined, thus transformed, into Al–Si eutectic-like particles.

Fig. 2 shows that the effectiveness of an ESV treatment conducted from 640 to 600 °C has a similar effect on the refinement of the microstructure to a treatment initiated at temperatures as high as 760 °C and ended at approximately 600 °C. This can be confirmed by comparing the respective SiML, 6.3 and 6.4, of both samples. Therefore, the temperature at which the ESV treatment ends is more important than the temperature at which the ESV treatment is initiated. The reason for this is the growth kinetics for the Si agglomerates in the liquid state and then the primary Si particles that coarse inversely to the temperature of the melt [23]. Therefore, ESV melt treatments are more effective when applied on alloys that have narrower range of temperatures between liquidus and the Al–Si eutectic nucleation $T_{E,NUC}^{Al-Si}$. The $T_{E,NUC}^{Al-Si}$ was reported as the end of the coarsening of the primary Si particles [30].

Comparing the microstructures shown in Fig. 2 for the treated samples using only chemical agents and the ESV treated samples it is clear that chemical agents have limited effect on microstructure refinement. For instance, the SiML are 4.3, 4.5 and 4.8 for the reference, chemically treated with P and chemically treated with P and Sr, respectively. In contrast, the SiML varies from 6.4 to 6.3. Nonetheless, it is clear that there is some effect on microstructure refinement with the use of chemical modifiers that is limited to a reduction in the size of the primary Si particles. Additionally, the additions of Sr further refined the eutectic-like Si particles (compare the values of SiML for the different samples in Fig. 2).

Combining ESV and chemical treatment result in the most efficient method to refine the microstructure. The additions of Sr for the ESV melt treated samples below the liquidus temperatures is highly effective and recommended for low cooling rates (~ 0.1 °C/s) as the ones used in the present research. The effectiveness of Sr is probably because at this point the ESV and P treatments have turned the Si agglomerates and primary Si particles are transformed into active sites for nucleation and are used for the Al–Si eutectic particles to continue their coarsening.

The SiML standard was selected because can be used to assess the level of modification of Si for microstructures of Al–Si hypo and hypereutectic alloys. For instance, the microstructure for the reference, chemically treated and ESV melt treated samples from 760 to 720 °C and from 760 to 680 °C (see Fig. 2) present combined primary Si particles and Al–Si eutectic particles. In contrast, the microstructures of the ESV and ESV + P + Sr treated samples at temperatures close or below liquidus (see Fig. 2) are primary Si free. The use of the well known AFS standard is limited to Al–Si hypoeutectic alloys and only considers the analysis of the Al–Si eutectic particles, therefore, is not adequate for the present investigation. For the above-mentioned reasons the SiML was selected in this research since is the only available standard that allows a direct comparison for any Al–Si 3XX alloy at any level of modification.

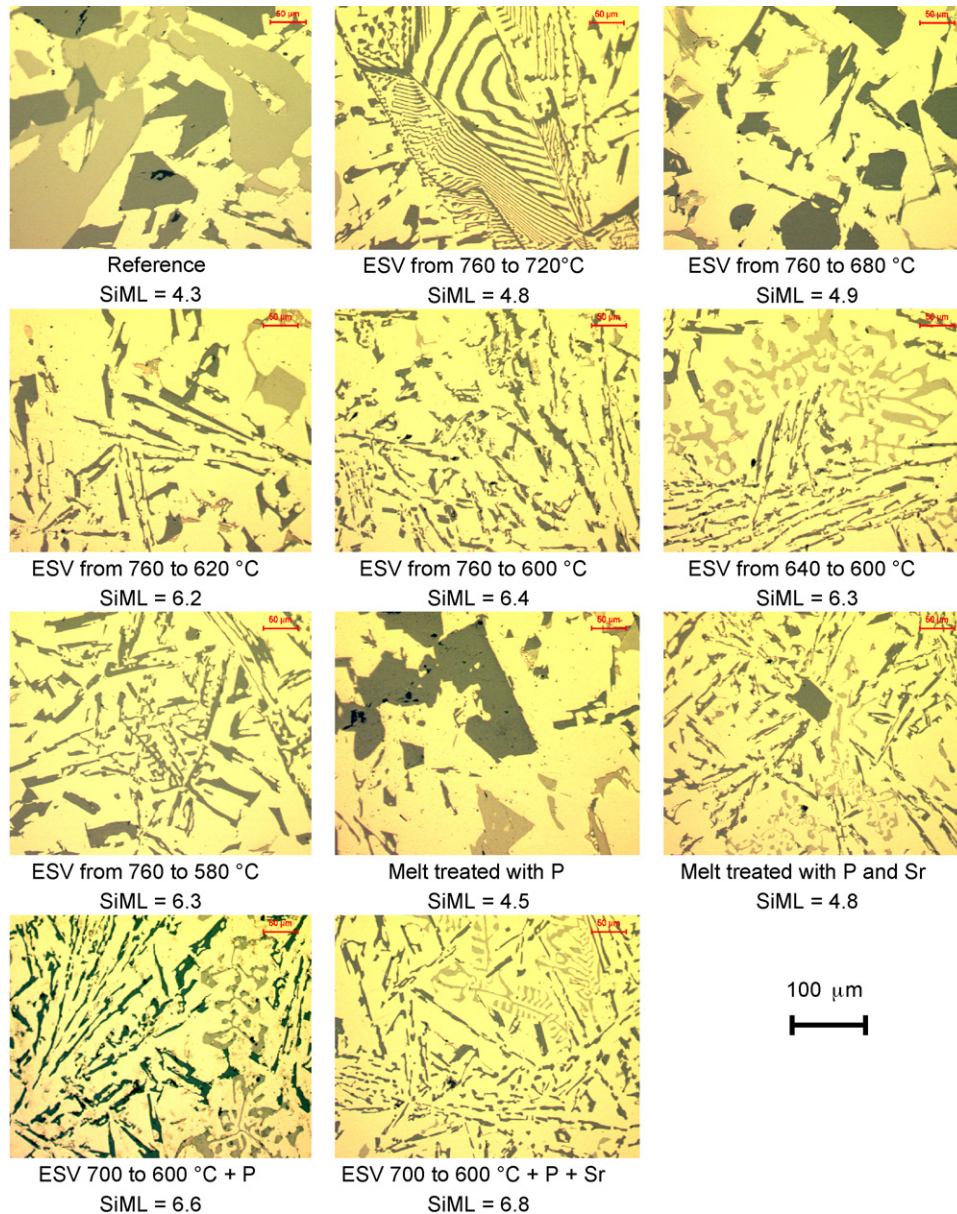


Fig. 2. Representative microstructures of the analytical samples cast under the conditions above indicated. In all cases, for the chemical treatments 60 ppm of P and Sr were added. The SiML [26] was used to assess the level of microstructure modification for the various 390 alloy investigated samples that were subjected to different melt treatments.

Table 2 shows the results of thermal analysis based as obtained from the cooling curve analysis. From Table 2 is observed a high consistency of the nucleation temperatures for the various reactions that allow us to conclude that the investigated samples have similar chemical composition. Unfortunately, there is no indication of a possible link among the nucleation temperature for any of the reactions and the level of refinement of the microstructure. Nonetheless, the analysis of the undercooling for the Al–Si eutectic ($\Delta T_E^{\text{Al-Si}}$) reaction has a clear path to the effect of the ESV and/or chemical treatment on the microstructure as shown in Fig. 3.

Fig. 3 shows sections of the cooling curves for selected samples treated under different conditions and indicates that the analysis of the $\Delta T_E^{\text{Al-Si}}$ can be implemented to monitor the effect of

the ESV treatment on microstructure. For instance, the $\Delta T_E^{\text{Al-Si}}$ for the ESV treated sample from 760 to 680 °C (short time and high temperature, thus limited modification) is comparable to the one presented by the reference sample (2.6 and 2.9 °C, respectively). In contrast, the $\Delta T_E^{\text{Al-Si}}$ for the sample treated from 700 to 600 °C was reduced to 0.43 °C (high modification) and a sample ESV treated in the same range of temperatures and chemically modified shows an almost neglected undercooling ($\Delta T_E^{\text{Al-Si}} = 0.08$ °C). Due to the high consistency of the $\Delta T_E^{\text{Al-Si}}$ with the SiML Eq. (5) was developed to be used as an algorithm to relate the $\Delta T_E^{\text{Al-Si}}$ with the level of microstructure refinement. Eq. (5) has a $R^2 = 0.94$ with the following confidence limits for 95% = ± 0.01 °C and for 99% = ± 0.002 °C and the $\Delta T_E^{\text{Al-Si}}$ is in °C. It is important to mention that Eq. (5)

Table 2
Principal solidification reactions and nucleation temperatures for the different phases identified during the solidification of 390 alloy as determined using thermal analysis

Sample	Solidification reaction					
	Primary Si	$T_{E,NUC}^{Al-Si}$	$T_{E,NUC}^{Mg_2Si}$	$T_{NUC}^{Al_3Ni}$	$T_{E,NUC}^{Al-Cu}$	T^{SOL}
Reference	632.3	567.8	536.1	521.0	502.0	481.9
760–720	630.6	566.2	536.9	525.3	501.9	478.6
760–680	634.7	569.2	536.6	521.4	502.7	483.3
760–620	634.5	569.1	538.5	521.3	501.8	481.8
700–600	630.2	572.2	536.5	521.2	502.2	480.3
640–600	634.7	569.8	538.8	521.2	502.4	480.9
760–580	633.5	569.6	538.7	520.4	502.7	477.2
Non-ESV ^a	634.6	571.0	536.1	521.2	501.8	478.5
Non-ESV ^b	636.4	567.9	539.4	521.1	502.6	480.1
700–600 ^b	628.6	573.0	538.3	521.9	503.4	484.3
700–600 ^a	631.7	568.1	537.5	520.1	502.0	482.7

The samples are classified based on the ESV and/or chemical treatment.

^a Samples chemically treated with 60 ppm of P

^b Samples chemically treated with 60 ppm of P + 60 ppm Sr.

is a mathematical model developed based on the results of the present research investigation with good chances to be extrapolated for other systems, but this topic has been contemplated for future publications.

$$SiML = 0.30(\Delta T_E^{Al-Si})^2 - 1.70(\Delta T_E^{Al-Si}) + 6.88 \quad (5)$$

The analysis of the undercooling for the Al–Si eutectic (ΔT_E^{Al-Si}) reaction is the best indicator for the level modification of Si. This is due to the fact that in order to nucleate a phase the temperature of the melt goes below the characteristic nucleation temperature of the phase in order to activate the sites for nucleation (in particular for alloys with equilibrium distribution coefficients ($k < 1$) and after the nucleation a recalescence effect is observed (see Fig. 3) [1,32]. The departure from the equilibrium temperature for nucleation is known as constitutional undercooling and has been widely investigated to relate the liquidus undercooling and the grain size for Al–Si hypoeutectic alloys ($k < 1$) [32].

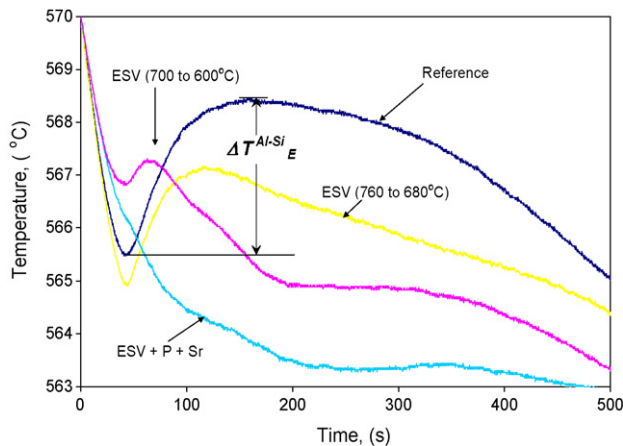


Fig. 3. Section of the cooling curve showing the effect of melt treatments, ESV and chemical, on the undercooling (ΔT_E^{Al-Si}) for the nucleation of the Al–Si eutectic reaction.

For a large undercooling coarse/large grains are expected and the grain size for a particular alloy decreases together with the constitutional undercooling. Similar phenomenon was reported by Djurdjevic et al. [33] for the analysis of the ΔT_E^{Al-Si} for Al–Si hypoeutectic alloys refined with Sr, which agrees with the analysis of the ΔT_E^{Al-Si} results in the present research. Therefore, the analysis of the ΔT_E^{Al-Si} to predict the level of Si modification is not limited to the chemical treatments and can be used for ESV and ESV + chemical treatments and also for Al–Si hypereutectic alloys. The analysis of the ΔT_E^{Al-Si} indicates that the lower the undercooling the finer the Si particles (primary and eutectic) in the microstructure that can be the result of a larger number of active sites for nucleation. Therefore, the decrease in the ΔT_E^{Al-Si} due to the use of the ESV or ESV + P + Sr melt treatments for the 390 alloys is due to the refinement of the Si agglomerates and primary Si particles. Probably every refined Si particle acts as an active site for coarsening for the Al–Si eutectic that resulted in a highly effective refinement methodology.

Fig. 4 shows the first derivatives of the cooling curves for the reference, ESV and ESV + chemically treated samples where the main solidification reactions and ESV melt treatment effect can be identified. Usually, samples solidifying under natural heat exchange conditions present exothermic reactions corresponding to the nucleation stage of the different phases and can be identified as peaks in the first derivative. Comparing the cooling curve and first derivatives the nucleation and growth of a solidification reaction can be recognized for a minimum (undercooling) and a maximum (recalescence), respectively (Fig. 3), or by an abrupt decrease of the cooling rate that form peaks in the first derivative corresponding. This effect is particularly evident in Fig. 4 for the T^{LIQ} and the ΔT_E^{Al-Si} solidification reactions. The primary Si solidification or liquidus does not present significant ΔT^{LIQ} , which could be due to the fact that primary Si particles are pre-nucleated at higher temperatures by the Si agglomerates [18,21–23]. Another possibility is fact that the 390 alloy is hypereutectic therefore has a $k > 1$ that has the opposite

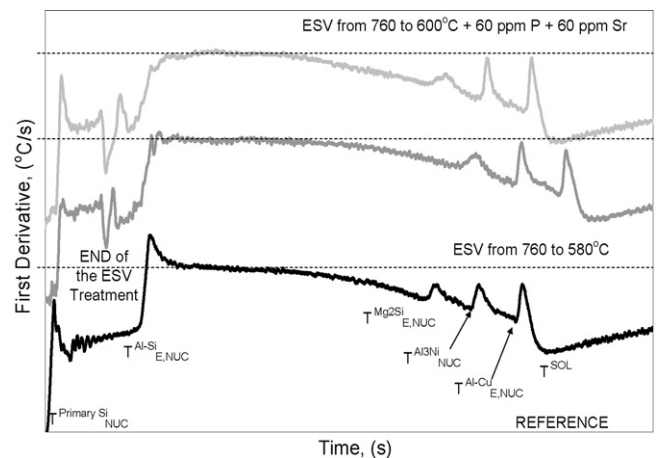


Fig. 4. First derivatives for the reference, ESV and ESV + chemically treated samples. For the three curves below the dotted “zero cooling rate” line, the cooling rate is negative (cooling) and above is positive (heating). Notice the decrease in recalescence as the level of Si modification increases (compare with the SiML in Fig. 2).

effect to the constitutional undercooling in comparison to an Al–Si hypoeutectic alloy [1,32]. Nonetheless, the first derivative shows the respective peak for this reaction. The nucleation of the Al–Si eutectic (Fig. 4; $T_{E,NUC}^{Al-Si}$) for the reference sample is highly exothermic and results in a drastic reduction of the cooling rate. The maximum of the peak for the reference sample goes to a positive cooling rate (due to a highly exothermic reaction effect, thus recalescence), meaning that at this point the sample is heating (Fig. 4; $T_{E,NUC}^{Al-Si}$) and the peak goes above the dotted line (*cero cooling rate*).

The cooling curves (Fig. 3) and first derivatives (Fig. 4) for treated and reference samples show significantly useful differences to predict the effect of melt treatment in microstructure refinement. Combining ESV and chemical treatments it is possible to minimize the ΔT_E^{Al-Si} avoiding the highly exothermic response or recalescence observed in the first derivative as a result the characteristic peak for this reaction only touches the “*cero cooling rate*” (dotted line). The low recalescence can be attributed to the neglected requirement for the activation of nucleation sites since they already exist as refined Si particles that are active sites for epitaxial growth for the Al–Si eutectic-like particles. The term eutectic-like is used in this research to refer the Si particles with Al–Si eutectic appearance that are present on ESV treated samples at temperatures close to liquidus.

Fig. 5 shows a hypothetical analysis to explain the growth (coarsening) of the Si particles followed by the reference, chemical, ESV and ESV + P melt treated samples. The objective of Fig. 5 is to propose a refinement mechanism for the Si particles as a function of the melt treatment. In a previous investigation was found that the growth (coarsening) of the Si agglomerates and primary Si particles is linear-like and the end of coarsening for the primary Si particles takes place at the $T_{E,NUC}^{Al-Si}$ [23]. Therefore, for the 390 alloy solidified under natural heat exchange conditions the coarsening of the Si particles starts from the already existing Si agglomerates that were never dissociated. In fact, the Si agglomerates are present at the casting temperature with

sizes of less than $200 \mu\text{m}^2$ [23]. From this temperature the Si agglomerates coarse freely to the $T_{E,NUC}^{Al-Si}$.

The determination of the effect of chemical modifiers or ESV melt treatments on the kinetics for coarsening of the Si particles is contemplated for future investigations. However, in the present investigation is proposed a theory, where is considered that melt treatments such as the ESV does not affect the diffusion rate of Si and the coarsening of the Si particles takes place from the end of the ESV melt treatment to the $T_{E,NUC}^{Al-Si}$ temperature. It is for this reason that in Fig. 5 the coarsening pathways are expressed with parallel lines for the reference, ESV and ESV + P melt treated samples. It is important to mention that these lines are hypothetical and do not necessarily represent the actual coarsening path of the primary Si particles. Also, the location where the SiML locations for the various samples investigated in this alloy is approximated and the Area of the primary Si particles was taken from literatures [23,24,30].

The use of a chemical modifier for the primary Si (such as P) has a multiplication effect of active sites for nucleation by promoting the formation of Si–Si covalent bonds [21]. The multiplication of the Si–Si bonds have a refining effect of the Si particles as shown in Fig. 5. However, the refining effect is limited to a small reduction in size of the Si agglomerates, since the heterogeneous nuclei (i.e. Al–P) has an initial size that depends on the size of the P particles contained in the Cu–8 wt% P master alloy. One of the main limitations when using only chemical agents is that the master alloys are usually applied at the casting temperature, which is from 150 to 200 °C above liquidus. Therefore, the time for coarsening of the primary Si particles depends directly from the time and temperature from the beginning of coarsening. Therefore, the coarsening for chemically treated alloys at the casting temperature is 200 °C higher than the ESV treated samples that are treated from the liquidus temperature. This itself reduces the coarsening of the Si particles in at least 150–200 °C, which results in an enhancing of the effects of ESV melt treatment over the chemical treatments (see Fig. 5). This can be translated in that for the chemical treatments the size of the Si agglomerates is reduced but the range of temperatures from casting to the $T_{E,NUC}^{Al-Si}$ is quite significant allowing a significant coarsening of the primary Si particles.

The ESV melt treatment has a more effective refining mechanism for two main reasons: the ESV melt treatment dissociates Si agglomerates creating very small coarsening sites for the Si particles and the end of the ESV treatment is close to the liquidus temperature that drastically narrows the range of temperatures for a limited coarsening (Fig. 5). The reason for the end of the ESV melt treatment at temperatures close to liquidus is because below this temperature start the fraction solid to increase and consequently the viscosity and strength increase considerably with temperature. This results in a drastic reduction on fluidity of the melt limits this technology to process such as rheocasting or thixocasting methods that were explored before [12,13,18].

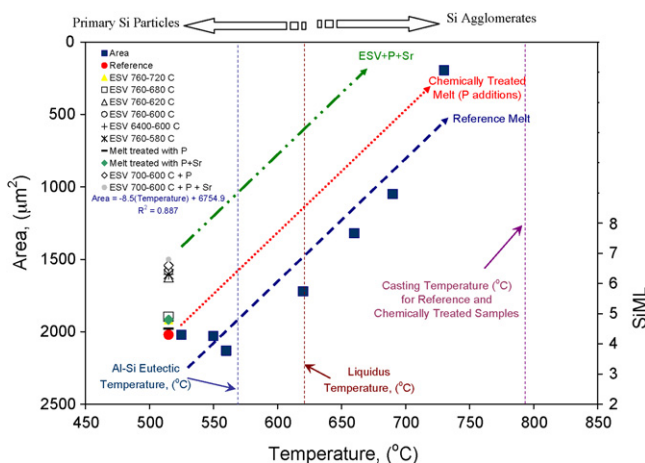


Fig. 5. Schematic representation of the coarsening of the Si agglomerates and the primary Si particles for Al–Si hypereutectic alloys that were solidified under natural heat exchange conditions and melt treated using chemical, electromagnetic stirring and vibration (ESV) and combined ESV and chemical melt treatments.

4. Conclusions

The use of melt treatments such as the ESV can be effective to modify microstructure of Al–Si hypereutectic alloys such as

the 390 particularly in the liquid state. ESV treatments applied at high temperatures ($\sim 100^\circ\text{C}$ above liquidus) promotes the formation of feathered-like primary Si particles however, at lower temperatures (close to the liquidus one) primary Si particles are refined more effectively, transforming them into Al–Si eutectic-like particles. The temperature at which the ESV treatment ends has more impact for the refinement of the Si particles than the initial temperature.

Chemical treatments alone have limited effect on microstructure refinement for the Al–Si hypereutectic alloys that in most cases is limited to the reduction in size of the primary Si particles. In contrast combining ESV and chemical treatments (adding P + Sr) resulted in the highest level of refinement of the microstructure for Al–Si hypereutectic alloys. The analysis of the $\Delta T_E^{\text{Al-Si}}$ in the cooling curve can be used to predict with a high accuracy ($R^2 = 0.94$) the level of microstructure modification using the SiML standard [30].

Acknowledgements

FCRH would like to thank the National Science and Technology Council (CONACyT) in Mexico for financial assistance during his Ph.D. studies. The authors would like to express their appreciation to the Natural Sciences & Eng. Research Council of Canada (NSERC).

References

- [1] J.E. Gruzleski, *Microstructure Development During Metalcasting*, first ed., AFS, Des Plaines, Illinois, 2000.
- [2] J. Campbell, *Castings*, Butterworth–Heinemann, 2003.
- [3] J.E. Gruzleski, *AFS Trans.* 9 (1994) 673.
- [4] F.C. Robles Hernandez, PhD Dissertation, University of Windsor, Canada (2004) p. 251.
- [5] S.D. McDonald, K. Noguira, A.K. Dahle, *Acta Mater.* 52 (2004) 473–4280.
- [6] P.S. Mohanty, J.E. Gruzleski, *Acta Mater.* 44 (1996) 3749–3760.
- [7] N. Saheby, T. Laouiz, A.R. Daudy, R. Yahayay, S. Radimany, *Philos. Mag. A* 82 (2004) 803–814.
- [8] P.J. Ward, H.V. Atkinson, P.R.G. Anderson, L.G. Elias, B. Garcia, L. Kahlen, J.M. Rodriguez-Ibabe, *Acta Mater.* 44 (1996) 1717–1727.
- [9] A. Sundarajan, A. Mortensen, T.Z. Katamis, M.C. Flemings, *Acta Mater.* 46 (1998) 91–99.
- [10] A.M. Kliauga, M. Ferrante, *Acta Mater.* 53 (2005) 345–356.
- [11] C. Vivès, *JOM* 50 (1998) 1–9.
- [12] C. Vivès, *Metall. Mater. Trans. B* 27B (1996) 457–464.
- [13] C. Vivès, *Metall. Mater. Trans. B* 23 (1992) 189–206.
- [14] I.G. Brodova, P.S. Popel, G.I. Eskin, *Liquid Metal Processing; Applications to Aluminium Alloy Production*, first ed., *Advances in Metallic Alloys*, New York, 2000.
- [15] A.K. Dahle, L. Arnberg, *Acta Mater.* 45 (1997) 547–559.
- [16] D.K. Sigworth, M.M. Guzowski, *AFS Trans.* 297 (1984) 907–912.
- [17] W.K. Kyffin, W.M. Rainforth, H.J. Jones, *J. Mater. Sci.* 36 (2001) 2667–2672.
- [18] J. Qiao, X. Song, X. Bian, L. Zhu, Q. Zhang, *Special Cast. Nonferrous Alloys* 43 (2002) 43–45.
- [19] J.L. Jorstad, *Modern Casting* 60 (1971) 59–64.
- [20] J.L. Jorstad, SDCE Paper No. 105, Detroit, MI, 1970.
- [21] B. Xiufang, W. Weimin, Q. Jimgyu, *Mater. Charact.* 46 (2001) 25–29.
- [22] G.I. Eskin, *Ultrasonic Treatment of Light Alloy Melts*, first ed., Gordon and Breach Science Press, 1998.
- [23] F.C. Robles Hernandez, J. H. Sokolowski, J. de J. Cruz Rivera, *Adv. Eng. Mater.*, 2006, in press.
- [24] F.C. Robles Hernandez, J.H. Sokolowski, *Adv. Eng. Mater.* 7 (11) (2005).
- [25] W. Weimin, B. Xiufang, J. Qin, S.I. Syliusarenko, *Metall. Mater. Trans.* 31A (2000) 2163–2168.
- [26] F.C. Robles Hernandez, M.B. Djurdjevic, W.T. Kierkus, J.H. Sokolowski, *Mater. Sci. Eng. A* 396 (2005) 271–276.
- [27] W. Weimin, B. Xiufang, J. Qin, *J. Mater. Sci. Lett.* 19 (2000) 1583–1585.
- [28] P. Xuemin, B. Xiufang, Z. Cheng, S. Jingqin, *Mater. Sci. Forum* 396–402 (2002) 119–124.
- [29] B. Xiufang, W. Weimin, *Mater. Lett.* 44 (2000) 54–58.
- [30] F.C. Robles Herández, J.H. Sokolowski, *J. Mat.* 57 (11) (2005).
- [31] M.H. Mulazimoglu, J.E. Gruzleski, *Aluminum* 69 (1993) 1014–1016.
- [32] M.A. Easton, D.H. StJohn, *Acta Mater.* 49 (2001) 1867–1878.
- [33] M.B. Djurdjevic, H. Jiang, J. Sokolowski, *Mater. Charact.* 46 (2001) 31–38.